



Evaluating the Neuroprotective Effects of Curcumin Nanoparticles on the Biochemical and Histological Alterations in Aluminum Chloride-Induced Alzheimer's Disease in rats



Akaber T. Keshta ^{*1}, Shaimaa A. Abdelrahman ², Alaa M. Alamin ¹

^{*1} Biochemistry Department, Faculty of Science, Zagazig University, PO Box-44519, Zagazig, Egypt

² Medical Histology and Cell Biology Department, Faculty of Medicine, Zagazig University, PO Box-44519, Zagazig, Egypt

Abstract

Alzheimer's disease (AD) has a significant financial impact on society since it is believed to be the most common neurological condition and one of the main causes of death for the elderly. Curcumin's remarkable pharmacological effects were hampered by its low bioavailability. Applying curcumin in its nanoform, which would enable it to traverse the blood-brain barrier, might help get over these restrictions. This current study aimed to investigate the neuroprotective effects of nanocurcumin on the AD induced by aluminum chloride "AlCl₃". 24 Swiss albino rats were divided into four groups; (I) negative control, group (II) diseased, group (III) protective, group (IV) therapeutic. At the end of experiment, behavioral test, assessment of biochemical markers, gene expression of neurogranin (RC3) and β -amyloid protein (APP), expression of phosphorylated Tau (p-Tau) and Glial fibrillary acidic protein (GFAP) immunohistochemically, and histopathological changes in the studied groups. Curcumin nanoform particles decreased the number of errors and the latency to escape box in the preventive and therapeutic groups. Furthermore, they reduced the oxidative stress induced by AlCl₃ in brain tissue, down-regulated the relative expression of APP, up-regulated of RC3 expression in hippocampus and improved the histopathological alterations in brain tissue. Curcumin coated with chitosan nanoparticles boosted drug permeability across the blood-brain barrier, boosted microglia activation, and accelerated the phagocytosis of the A β peptide, suggests that curcumin was among the most intriguing and promising compounds for developing therapies for AD. Additionally, neurogranin as a post-synaptic membrane protein can be a promising tool for early diagnosis of cognitive decline.

Keywords: Alzheimer's disease; Curcumin nanoform; neurogranin; β -amyloid protein; blood-brain barrier; Neuroprotective.

1. Introduction

Alzheimer's disease (AD) is an incurable neurological condition that causes a progressive decline in cognitive functioning, including memory loss, language difficulties, and difficulties with judgment and understanding [1]. In 2010, 16.2% of the world population consisted of people aged 65 or over, a figure that is expected to rise up to 26.9% by 2050. Increasing life expectancy highlights the importance of physical and mental health in old age [2]. The pre-clinical stage, which is the initial clinical phase of AD, is sometimes referred to as the pre-symptomatic stage and can last for several years or more. At this point, there are no clinical indications or symptoms of AD, no mild memory loss, no early pathological changes in the brain and hippocampus, and no functional impairment in day-to-day activities [3]. The early stage of AD is when many symptoms first appear in patients. These symptoms include mood swings, the beginning of depression, difficulty adjusting to daily life owing to memory loss and attention challenges, and confusion regarding place and time [4]. Moderate stage in which the disease spreads to different areas of the cerebral cortex, it results in more severe memory loss, which includes issues identifying friends and family, losing impulse control, and experiencing difficulty speaking, writing, and reading [3]. Severe AD, also known as late-stage AD, is characterized by a progressive loss of function and cognition, including the inability to recognize family members, bedridden status, problems swallowing and urinating, and ultimately, the patient's death from these complications. The disease spreads throughout the entire cortex area with a severe accumulation of neurotic plaques and neurofibrillary tangles [5]. There are several theories explaining AD, but only two are considered to be major: one suggests that modifications in the production and processing of amyloid β -protein (APP) are the main cause of the disease, while others argue that cholinergic dysfunction is a significant risk factor [1]. Aging, genetics, brain trauma, vascular illnesses, infections, and environmental variables (heavy metals, trace metals, and others) have all been linked to AD, which is thought to be a complex disease. Aluminum (Al) builds up in the parts of the brain, hippocampus, and cerebellum where it interacts with proteins to phosphorylate highly phosphorylated proteins such as tau protein, which is indicative of AD [6]. Elevated Al concentrations in AD are linked to degeneration, oxidative stress, neuronal death, and changes in neurotransmission. High exposure to Al causes neurofibrillary degeneration [7]. It is well known that this metal accelerates the production and

*Corresponding author e-mail: at_keshta2004@yahoo.com; (Akaber T. Keshta).

Receive Date: 06 May 2024, Revise Date: 12 June 2024, Accept Date: 25 June 2024

DOI: 10.21608/ejchem.2024.287556.9679

©2025 National Information and Documentation Center (NIDOC)

aggregation of extracellular β amyloid [8]. Asian cuisine frequently uses the root turmeric (*Curcuma longa*) as a spice due to its many therapeutic benefits, which include anti-inflammatory, antioxidant, anti-HIV, antibacterial, anti-tumor, and restorative effects on the brain-derived neurotrophic factor (BDNF) [9]. Although curcumin, a polyphenol, has numerous biological effects, it is not highly soluble in water. Its low bioavailability is caused by its rapid metabolism, rapid systemic clearance, and restricted absorption [10]. The synthesis of hydrophobic medications at the nanoscale improves their solubility and bioavailability. Additionally, medications that are nano-sized can readily enter cells and target specific cytosolic regions, such as those containing proteins, nucleic acids, and other small molecules [11]. Curcumin nano-formulations have revolutionized the treatment of diseases by improving cellular absorption, permeability with increased plasma levels, and bioavailability [12]. Curcumin nanoparticles (CNs) have the potential to improve bioavailability, biological half-life, tissue distribution, and clinical application efficacy [13]. The goal of the current study was to assess nanocurcumin's potential for amelioration in a rat model of Alzheimer's disease caused by $AlCl_3$. This could be accomplished by investigating the different mechanisms that underlie the biochemical and histological alterations that take place in the groups under study.

2. Results and Discussion

2.1. Results

2.1.1. Scanning Electron Microscopy (SEM) of Curcumin Nanoparticles

The SEM image showed that the nanoparticles were made up of many crystallites with rutile structures. Based on SEM scans, the curcumin nanoparticles in Fig. (1) below ranged in size from less than 100 nm and were roughly spherical.

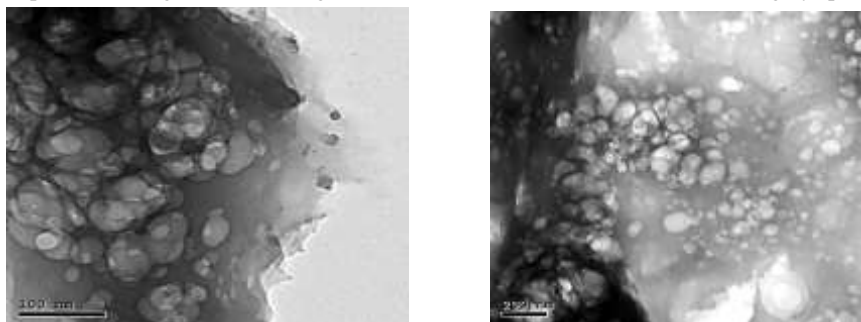


Fig. 1: SEM images of Cur@Chitosan nanoparticles with average size <100 nm.

2.1.2. Behavioral data [Barnes maze test (Cognitive changes)]:

The AD group (group II) spent less time in the target quarter on test day and made more mistakes during training and the test, according to the results of the Barnes maze test. Furthermore, group II took longer on the first and second training days to recognize the escape box. These findings suggest that the AD process slowed down memory and recall. The protected and treated groups showed a significant increase in time spent as well as a significant decrease in the number of errors on training and test days compared to the AD group. Meanwhile, group III, the protected group, had a significant improvement over the treated group (IV). Trials from the AT2–AT6 groups demonstrated improved performance in both the protected and treated groups, as Table (1) demonstrated. The diseased rats had a higher latency to escape box from AT1–AT6, ranging from 249.38 ± 31.68 to 111.44 ± 27.87 , in comparison to the control group's (82.04 ± 26.82 — 10.82 ± 2.38). It required less time for the treated group (154.09 ± 30.43 — 40.99 ± 19.31) and the protected group (91.44 ± 10.55 — 17.91 ± 5.08) to reach the escape box ($p < 0.001$) Table (2) error numbers were as follows: the diseased group had the greatest average error score (8.83 ± 0.98 — 4.67 ± 0.52), compared to control group's average errors, ranging from (3 ± 1.10 — 2.17 ± 1.6) from AT1 to AT6. Rats in the protected group make fewer errors overall, with AT1–AT6 ranging from (4.17 ± 1.6 — 2.5 ± 0.55), while the average errors in the treated group range from (6.5 ± 1.38 — 3 ± 1.79), ($p < 0.001$).

Table 1: Latency to escape in all the studied groups at different trails by seconds

	Group I (Control)	Group II (Diseased)	Group III (Protected)	Group IV (Treated)
AT1	82.04 ± 26.82	249.38 ± 31.68^A	91.44 ± 10.55^B	$154.09 \pm 30.43^{a,B,c}$
AT2	33.67 ± 8.10	210.18 ± 22.58^A	47.41 ± 9.67^B	$70.90 \pm 2.88^{A,B,c}$
AT3	66.72 ± 8.52	235.14 ± 30.34^A	73.50 ± 13.59^B	$92.09 \pm 20.99^{a,B}$
AT4	26.64 ± 9.89	209.31 ± 13.63^A	43.58 ± 10.07^B	$66.64 \pm 8.91^{A,B,c}$
AT5	16.13 ± 2.66	156.06 ± 41.17^A	$32.18 \pm 1.66^{A,B}$	$49.34 \pm 1.03^{A,B}$
AT6	10.82 ± 2.38	111.44 ± 27.87^A	17.91 ± 5.08^B	$40.99 \pm 19.31^{A,B,C}$

**: highly significant ($p < 0.001$) Post hoc: Tukey test ^a: significant versus control, ^A: Highly significant versus control, ^b: significant versus diseased, ^B: Highly significant versus diseased, ^c: significant versus protected, ^C: Highly significant versus protected. [p value < 0.0001].

Table 2: Number of errors in all the studied groups at different trails

	Group I (Control)	Group II (Diseased)	Group III (Protected)	Group IV (Treated)	P
AT1	3±1.10	8.83±0.98 ^A	4.17±1.6 ^B	6.5±1.38 ^{a,b,c}	<0.001**
AT2	2.67±0.82	5.83±1.17 ^a	3.67±1.21 ^b	4.5±1.76 ^A	0.003*
AT3	3.83±1.17	8±1.26 ^a	6.17±1.72 ^{a,b}	6.67±2.73 ^a	0.007*
AT4	1.67±0.52	4.5±1.64 ^a	3.5±1.97 ^a	4±1.79 ^a	0.03*
AT5	2.33±1.37	5.83±0.98 ^A	4.5±1.52 ^a	4.67±0.82 ^a	0.001*
AT6	2.17±1.6	4.67±0.52 ^a	2.5±0.55	3±1.79	0.01*

** : highly significant ($p < 0.001$) Post hoc: Tukey test ^a: significant versus control, ^A: Highly significant versus control, ^b: significant versus diseased, ^B: Highly significant versus diseased, ^c: significant versus protected, ^C: Highly significant versus protected. [p value < 0.0001].

The diseased group in Probe Trial (PT1) had a considerably greater escape hole latency than all other groups ($p < 0.001$), whereas the protected group scored less time after the control group. The rats in the control group scored 31.35±17 in the PT1 latency to escape hole, whereas the rats in the diseased group took longer at 119.99±59.08, and the rats in the protected group scored 47.05±9.57 and the treated group scored 91.21±12.67. All groups differed considerably from each other ($p < 0.001$).

The rats in the PT2 control group took an average of 29.55±16, whereas the rats in the diseased group took 104.19±27.42, and the rats in the protected group took less time—32.11±1.41—and the treated group took 95.49±6.64—than in the other groups ($p < 0.001$) Table (3) [a, and b].

Table 3: [a]: Latency to escape in all the studied groups at different Probe trials by seconds

	Group I (Control)	Group II (Diseased)	Group III (Protected)	Group IV (Treated)	P
PT1	31.35±17.86	119.99±59.08 ^A	47.05±9.57 ^B	91.21±12.67 ^{A,b,c}	<0.001**
PT2	29.55±16.64	104.19±27.42 ^A	32.11±1.41 ^B	95.49±6.64 ^{A,C}	<0.001**

Table 3: [b]: Number of Errors in all the studied groups at different Probe trials by seconds

	Group I (Control)	Group II (Diseased)	Group III (Protected)	Group IV (Treated)	P
PT1	1±0.89	5±1.26 ^A	1.67±52 ^B	2±0 ^{a,B}	<0.001**
PT2	0.33±0.52	4.17±2.31 ^A	0.67±0.52 ^B	2±1.96 ^{a,b,c}	<0.001**

** : highly significant ($p < 0.001$) Post hoc: Tukey test ^a: significant versus control, ^A: Highly significant versus control, ^b: significant versus diseased, ^B: Highly significant versus diseased, ^c: significant versus protected, ^C: Highly significant versus protected. [p value < 0.0001].

2.1.3. Effect of nanocurcumin particles on antioxidants in the studied groups

Table (4) recorded the effect of nanocurcumin on the oxidative and antioxidants levels (GSH, CAT, and SOD) in the tissue homogenate. The GSH levels in group II was significantly reduced (4.01 ± 0.19 mg/ g tissue) compared to the GSH levels in control group (16.53 ± 0.72), and significantly increased in both protective and treated groups, [(10.36 ± 0.48) and (6.49 ± 0.31)]; respectively compared to group II (AD group), ($p < 0.0001$). CAT activities revealed a significant reduction from (445.35 ± 23.62 U/ g tissue) in negative control group to (85.1 ± 4.59) in group II, meanwhile these activities were significantly increased to (278.85 ± 13.62) in protective group and to (157.69 ± 7.80) in treated group, compared group II, ($p < 0.0001$). SOD activities were found to be (65.29 ± 2.33 U/ g tissue) in group I, these activities were suppressed in group II to (30.06 ± 1.57). while these activities were elevated in both protective and treated groups to (55.62 ± 2.15), and (43.11 ± 2.06); respectively, ($p < 0.001$) compared to group II.

Table 4: The effect of nanocurcumin on antioxidants markers in tissue homogenate

Groups	GSH (mg/ g tissue)	CAT (U/ g tissue)	SOD (U/ g tissue)	
Group I	16.53±0.72	445.35 ± 23.62	65.29±2.33	
Group II	4.01±0.19	85.1±4.59	30.06±1.57	<i>p</i> < 0.0001**
Group III	10.36±0.48	278.85± 13.62	55.62±2.15	
Group IV	6.49±0.31	157.69± 7.80	43.11±2.06	

***: highly significant ($p < 0.0001$) Post hoc: Tukey test. All 4 means are significantly different from one another.

2.1.4. Effect of nanocurcumin particles on AChE activity

AChE activity was decreased from (7.83±0.38 U/ g tissue) in group I to 3.25 ±0.13 in group II. Meanwhile, these activities were increased to 6.41±0.30 in group III and to 4.75±0.19 in group IV compared to group II, ($p < 0.001$), as reported in table (5).

Table 5: The effect of nanocurcumin on antioxidants markers in tissue homogenate

Groups	AChE activity (U/ g tissue)	
Group I	7.83±0.38	<i>p</i> < 0.0001**
Group II	3.25±0.13	
Group III	6.41±0.30	
Group IV	4.75±0.19	

***: highly significant ($p < 0.0001$) Post hoc: Tukey test. All 4 means are significantly different from one another.

2.1.5. Relative expression of β -amyloid & Neurogranin genes

Results were illustrated in Fig. (2). On a hand; the mean value of β amyloid gene expression in AD diseased group (16.11± 0.86) was significantly increased compared to its corresponding values in negative control group (1.00±0.00). While, the β amyloid gene expression was decreased in both protective and treated groups (3.66±0.16), and (7.11± 0.36); respectively.

On the other hand, Neurogranin expression (RC3 or Ng) gene was reduced from (9.45±0.43) in control group to (1.0± 0.01) in AD diseased group. But the gene expression was elevated in both protective and treated groups to (6.11±0.31), and (2.33±0.12); respectively compared to diseased group. Fig. (3).

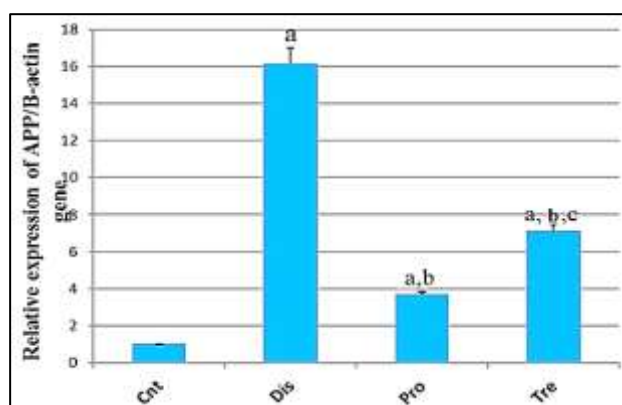


Fig. (2) Relative gene expression of β amyloid gene in different studied groups. [Data are presented as mean ± SD. a: significant with group I, b: significant with group II, c: significant with group III].

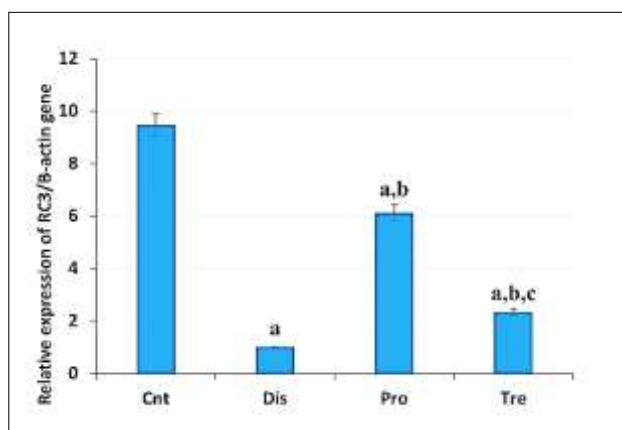


Fig.(3) Relative gene expression of Neurogranin (RC3) gene in different studied groups. [Data are presented as mean \pm SD. a: significant with group I, b: significant with group II, c: significant with group III].

2.1.6. Histological results

H&E-stained sections from the control group showed the hippocampal formation was formed of the Cornu Ammonis (CA) regions; CA1, CA2, CA3, CA4 and Dentate gyrus (DG) Fig. (4a). The dentate gyrus was formed of molecular, granular, and polymorphic layers. The granular layer was composed of densely packed granule cells with vesicular nuclei. Neuroglial cells and blood capillaries were seen in polymorphic and molecular layers Fig. (4b). Group II showed markedly distorted hippocampal regions. The dentate gyrus showed marked cell loss in granular layer and many granule cells showed dark apoptotic nuclei. Extensive vacuolations were evident in all regions of DG Fig. (4c). Group III showed the granular layer contained many granule cells with vesicular nuclei. The sub-granular zone showed small cells with dark nuclei. Neuroglial cells and blood capillaries were seen in Polymorphic and Molecular layers (Fig. 4d). H&E- stained sections of group IV showed the granular layer of DG showed few cells with pale vesicular nuclei and many cells appeared shrunken with dark nuclei. Polymorphic and Molecular layers showed neuroglial cells and blood capillaries Fig.(4e).

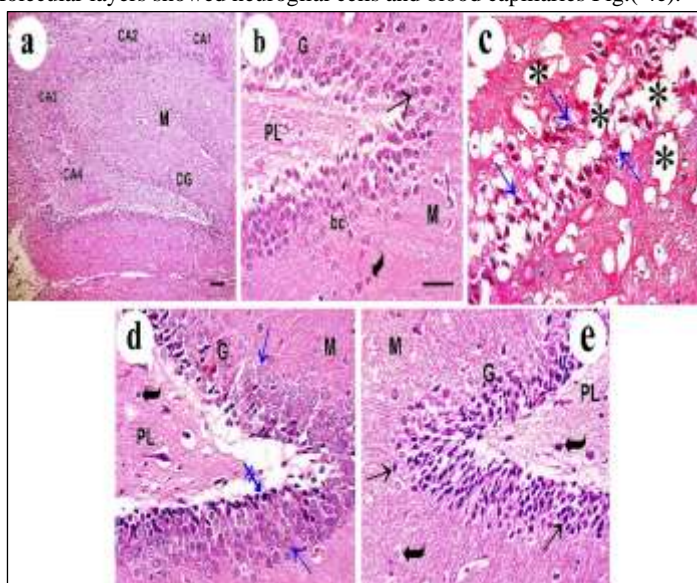


Fig. 4: (a) H&E-stained section from the control group showing The hippocampus is formed of the Cornu Ammonis (CA) regions; CA1, CA2, CA3, CA4 and Dentate gyrus (DG). Molecular layer (M) separates CA regions from DG. (b) the higher magnification of the same group showing normal architecture of the dentate gyrus which is formed of molecular (M), granular (G), and polymorphic (PL) layers. The granular layer contains granule cells (arrow) with vesicular nuclei. Polymorphic and molecular layers contain neuroglial cells (curved arrow) and blood capillaries (bc). (c) group II shows marked cell loss and most granule cells have apoptotic nuclei (arrow). Extensive vacuolation (asterisks) are seen in all regions. (d) group III shows normal appearance of the dentate gyrus as many granule cells have vesicular nuclei (arrow), few cells have dark apoptotic nuclei (crossed arrow). Normal shaped molecular (M) and polymorphic layers (PL) with neuroglial cells (curved arrow). (e) group IV shows many cells of the granular layer (G) are shrunken with dark apoptotic nuclei (arrow). Polymorphic (PL) and Molecular (M) layers show few neuroglial cells (curved arrow) (H&E stain: a x100 Scale bar 50 μ m, b-e x400 Scale bar 30 μ m)

2.1.7. Immunohistochemical results

Immunohistochemical stained sections for GFAP showed brown cytoplasmic expression in cell bodies and processes of astrocytes of control group I. Marked increase in the number of astrocytes with increased intensity of immune expression appeared in the cytoplasm and processes of astrocytes in all layers of group II. Brown cytoplasmic expression appeared in astrocytes of groups III with an apparently decreased number of astrocytes than group II. Moreover, moderate brown expression of GFAP also appeared in astrocytes cytoplasm and processes of groups IV Fig. (5).

Immunohistochemical-stained sections for anti p-Tau antibody revealed faint brown staining of the perikaryal cytoplasm of the neuronal cell bodies and their apical dendrites that appeared as long thin threads in the ML of DG of group I. Group II showed strong expression of p-Tau that appeared as dark brown staining of the neuronal cells' cytoplasm and their apical dendrites which appeared as thick disrupted threads in the ML. Group III displayed faint expression of p-Tau in neuronal cells cytoplasm and processes. Group IV revealed moderate expression of p-Tau that appeared as moderate brown staining of neuronal cytoplasm and their apical dendrites Fig. (5).

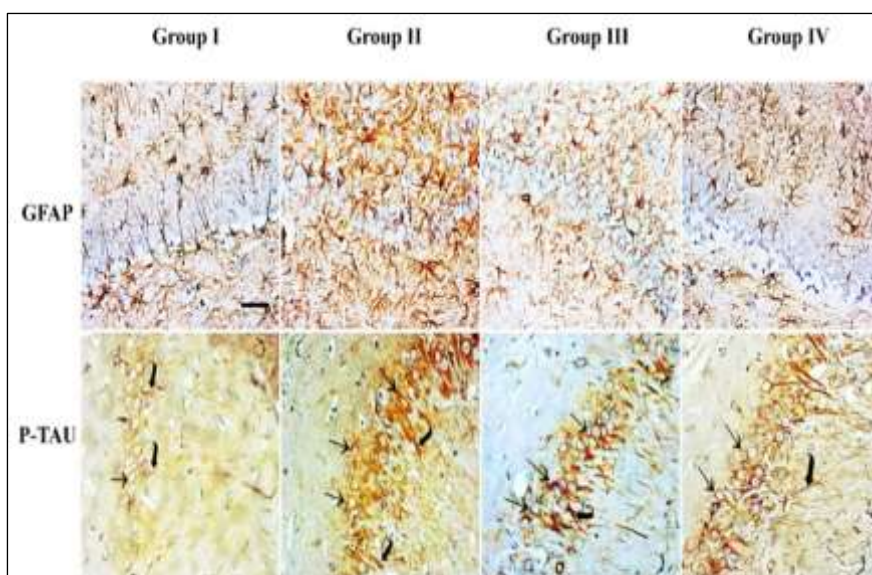


Fig. (5): Immunohistochemical staining with anti- GFAP antibody shows brown cytoplasmic expression in cell bodies and processes of astrocytes of control group I. Marked increase in the number of astrocytes with increased intensity of immune expression is shown in cytoplasm and processes of astrocytes in all layers of group II. Decreased number and intensity of immune expression is shown in cytoplasm and processes of astrocytes in all layers of group III. Group IV shows brown expression in cytoplasm and processes of many astrocytes. Immunohistochemical staining of p-Tau in the hippocampus of the control group shows faint brown staining of the perikaryon cytoplasm (arrow) of the neuronal cell bodies and their processes that appear as long thin threads (curved arrow). Group II exhibits an intense brown staining of the perikaryon cytoplasm (arrow) of the neuronal cell bodies and their processes (curved arrow). Group III reveals faint brown staining of the perikaryon cytoplasm (arrow) of the neuronal cell bodies and their processes (curved arrow). Group IV reveals a moderate brown staining of the perikaryal cytoplasm (arrow) the neuronal cell bodies and their processes (curved arrow). (Avidin biotin Peroxidase system X400, Scale bar 30 μ m).

2.1.8. Morphometric results of histopathological examination of different studied groups

The mean area % of GFAP and P-TAU immune-expression in AD group (Group II) were highly significantly increased in hippocampus compared to control group ($p < 0.0001$); but significantly decreased in both protected and treated groups with marked improvement was noticed in group III. Group IV showed highly significant difference from other groups ($p < 0.0001$) Figs. (6), (7); respectively.

2.2. Discussion

The most prevalent type of dementia is Alzheimer's disease (AD), a multifactorial neurodegenerative central nervous system illness that is highly prevalent among the elderly [14]. Extracellular plaques made of amyloid β ($A\beta$) or neurofibrillary tangles (NFT) and hyper-phosphorylated tau are the two primary pathogenic characteristics of AD [15].

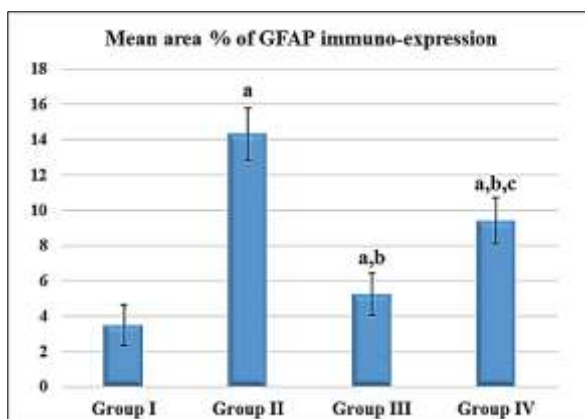


Fig. (6): Mean area % of GFAP immune-expression in the different groups

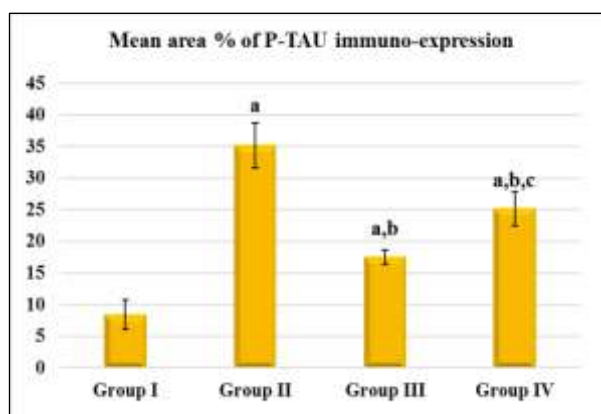


Fig. (7): Mean area % of P-TAU immune-expression in the different groups

$A\beta$ aggregation, leading to neuronal death and dementia. Under normal conditions, tau proteins stabilize the microtubule; however, accumulation, aggregation, and neurotoxicity occur when these proteins are cleaved or hyper-phosphorylated. AD group performed the worst in recognition and learning during training when compared to the control one. However, after receiving nanocurcumin treatment in groups III and IV, the rats performed better in both recognition and learning. Increased concentrations of Aluminum (Al) have been connected to degeneration, oxidative stress, neuronal death, and alterations in neurotransmission in AD. Al is a metal commonly acknowledged to be a neurotoxic. There is neurofibrillary degeneration due to high Al exposure [16]. $AlCl_3$ caused a considerable impairment in memory in the step-down apparatus at subsequent times, as indicated by the animal's latency time and the quantity of errors it made during the trial [17].

It has been reported that Al administration increases the expression of $A\beta$ (1–42), β and γ -secretases in the hippocampus and cortex of rats, suggesting that Al toxicity leads to the $A\beta$ formation [18]. AD is characterized by a gradual loss of neuronal function, memory loss, and a decline in language skills [19]. AD affects memory, thought, and language processes.

Curcuma longa rhizome contains the hydrophobic bioactive component curcumin (diferuloylmethane). Because of its diverse biological and pharmacological actions, it has garnered a great deal of study. Its quick metabolism, limited water solubility, and poor bioavailability, however, are significant obstacles to its beneficial medicinal uses. Curcumin's biological and pharmacological advantages are increased by nano-range formulations, or Nanocurcumin, which was not before considerably achievable [13].

Benefits of curcumin therapy for cognitive impairments and neuropsychiatric diseases [20]. Curcumin therapy had an effect on spatial learning memory (as judged by the Barnes Maze), long-term memory (LTM), or short-term memory (STM) in the item identification test [21]. Through an increase in spontaneous alternation of behavior, rats treated with curcumin

showed a considerable reduction in the damage caused by beta-amyloid deposition, all without increasing the number of maze entries [9].

Our findings also demonstrated that, in comparison to the control group and other groups, exposure to $AlCl_3$ reduced the levels of GSH, CAT and SOD activities in diseased group where these activities were elevated in both protective and treated groups compared to diseased one. One major danger to AD is oxidative stress. Redox abnormalities are thought to have a role in the neurodegenerative process that results in the impairment that reactive oxygen species (ROS) and reactive nitrogen species (RNS) mediate in the brains of AD patients. Natural antioxidants are thought to protect neurons [8].

ROS induction caused neurotoxicity when Al accumulated in the hippocampal tissues [22]. $A\beta$ deposition causes glial cells to emit pro-inflammatory cytokines, cyclooxygenase, and raise levels of ROS and cellular damage. Two types of free radicals that can be generated when $A\beta$ peptides activate glia's NADPH oxidase are superoxide and hydrogen peroxide [23].

Nanocurcumin can cross the blood-brain barrier (BBB) to enter brain tissue, where it concentrates chiefly in the hippocampus and for a significantly prolonged retention time in the cerebral cortex (increased by 96%) and hippocampus (increased by 83%) [24].

Curcumin demonstrates potent antioxidant characteristics. Transition metal chelation, a well-known antioxidant process found in curcumin, is linked to the *o*-methoxy and diketone phenol moieties. It has the ability to scavenge free radicals like ROS and RNS in addition to regulating the activity of the enzymes catalase, and SOD to neutralize the free radicals. Curcumin nanoparticles used its antioxidant effect to lessen lipid peroxidation and enhance the functions of detoxifying and antioxidant enzymes to prevent damage to the circulatory system [25]. Additionally, curcumin inhibits lipoxygenase and cyclooxygenase, two enzymes that generate reactive oxygen species [26]. Our findings corroborated those of Kahya et al., [27], who reported that injecting $AlCl_3$ decreased GSH and CAT activity. Also, using curcumin nanoparticles, rats' oxidative stress was significantly reduced [28].

AD group showed a reduction in AChE activity compared to group I. While, the protected and treated groups recorded increase in AChE activity. AD patients exhibit lower AChE activity along with a concomitant decline in cognitive abilities. After intraperitoneal injection of $AlCl_3$, there was a decrease in cholinergic activity, a formation of free radicals, and cognitive dysfunction, which were all linked to the disruption of cellular oxidant anti-oxidant defense [17]. In both cholinergic and cholinceptive (non-cholinergic) neurons, acetylcholinesterase is present. It has been observed that in areas of the cortex where there is a significant loss of acetylcholinesterase-rich axons, individuals with AD may have an almost normal density of acetylcholinesterase-rich cholinceptive perikarya. Therefore, ligands that represent acetylcholine production rather than acetylcholinesterase activity may be more helpful in the early identification of AD [29]. The loss of neurons and synapses, aberrant neurotransmitter metabolism, and dysfunctional autophagy are among the other primary indicators of AD [30].

Curcumin considerably increased memory retention, decreased oxidative damage, changed acetylcholinesterase activity, and decreased aluminum concentrations, all of which showed a neuroprotective effect against cognitive impairment and aluminum-induced oxidative stress [9]. The investigation's current findings align with results of Sakly [31] and Lakshmi et al., [32] who reported that, the brain's cortex and hippocampus regions experience cholinergic fiber degradation and AChE depletion as a result of chronic aluminum treatment. The relative expression of β -amyloid gene in the current study recorded a highly significant elevation in group II while, protected and treated groups these levels of expression were reduced. Excessive $A\beta$ plaque buildup at many brain locations is a pathogenic feature of AD. $A\beta$ plaques are either more common or present in an aggregation-prone state. $A\beta$ accumulation caused a range of microglia-activated neuroinflammations, which is one of the primary markers of AD [33].

Neurogranin (RC3 or Ng) is a protein unique to neurons that binds to calmodulin post-synaptically. It is highly expressed in the brain, particularly in the hippocampus's dendritic spine and cerebral cortex. It is postulated that it influences synaptic plasticity and long-term potentiation (LTP) by regulating calcium-mediated signaling pathways. Unlike traditional biomarkers, Ng can detect the degenerative changes of AD early. It has high levels of neuronal expression in the central nervous system. Ng exhibited a robust association with the amyloid concentration [34]. Ng binding to calmodulin weakened when the synaptic structure is disrupted, affecting the transmission of Ca^{2+} between the synapses and the formation of LTP, thus it leads to early cognitive decline. It might provide thorough guidance on managing AD. It may also yield important information for monitoring the course of the illness over an extended period of time and assessing how drugs affect synaptic degeneration in AD clinical trials [35].

It was previously believed that long-term Al treatment produced reactive oxygen species in the brain, which led to neurotoxicity. Iron-induced oxidative stress in the central nervous system (CNS), brought on by Al buildup, stimulates amyloidogenic fragments, NFTs, and neuro-inflammatory cytokines [36]. Curcumin NPs have the potential to greatly enhance spatial learning and memory by reducing excessive Tau protein phosphorylation and hippocampus $A\beta$ formation. They discovered that the NPs could quickly and efficiently speed up the phagocytosis of $A\beta_{42}$, stimulate microglia activation, and enhance medication penetration through the BBB [37].

The findings of Eghbaliferiz et al., [38], who demonstrated the substance's neurological action by binding to senile plaques and preventing amyloid plaque aggregation, were consistent with our findings. Consistent with our findings, Saunders et al., [39] observed a noteworthy reduction in Ng (RC3) in brain tissue homogenate from AD cases compared to healthy aging controls and midlife's. The decrease in Ng levels between AD and healthy agers was corroborated by gene expression results, which also revealed that AD had significantly lower Ng (RC3) levels than healthy agers. Age-related decreases in Ng protein mRNA expression were observed in rodents. Concerning the immunohistochemistry results, p-Tau was strongly expressed in our study and manifested as thick disrupted threads and dark brown staining of the neuronal cells in group II. Following the

administration of nanocurcumin to group III, group IV showed moderate expression of p-Tau in neuronal cells, while group III showed faint expression.

Tau has been found to be localized to both synaptic compartments in control and AD tissue in earlier postmortem investigations involving analysis of synaptosomes and synaptic fractions of homogenized tissue [40]. While neurofibrillary tangles, which are formed after hyper-phosphorylation of microtubule-associated protein tau, are well correlated with cognitive impairment, dementia, and neurodegeneration in AD, a study by Akhtar et al., [41] demonstrated that A β peptide aggregates result in the formation of senile plaques [42]. Curcumin's nanoparticles were able to significantly down-regulate or block the p-tau deposition; this effect was further amplified by curcumin's nano delivery. This suggests that curcumin can reduce neurotoxic substances like p-tau that are elevated in the AD brain [43].

In comparison to the control group, our study demonstrated a significant increase in the quantity of astrocytes exhibiting heightened immune expression in the cytoplasm and processes in AD group II. In the central nervous system, astrocytes are the only cells that express a high level of Glial Fibrillary Acidic Protein (GFAP) [44]. In AD, there has been evidence of increased GFAP in brain tissue. The immune-expression levels of GFAP were improved by curcumin supplementation exhibiting lower levels [45].

A correlation was found between a high level of GFAP in the temporal and parietal cortices during autopsy and poor cognitive function in later life [46]. Adults with symptomatic AD who had higher levels of GFAP also had worse verbal episodic memory [47]. Curcumin directly inhibits astrocyte activity in neurodegenerative diseases and ischemic stroke, according to recent research. The fundamental processes of migration and neuroinflammation in the activated astrocytes are still unclear [38, and 48]. The observed amelioration in astrocytes expression levels could be explained by the anti-inflammatory and anti-oxidant effects of nanocurcumin as proved by the results of the present study.

3. Experimental

3.1.1. Chemicals

Aluminum Chloride 98% (AlCl₃), Curcumin powder, were purchased from Sigma–Aldrich (UK). CAS No: 7446-70-0, LOT No: BCCB0771, and CAS No: 458-37-7; respectively.

Antioxidants kits [Glutathione reduced (GSH), catalase (CAT), superoxide dismutase (SOD)] were purchased from (Bio-diagnostic company, Egypt) CAT. No: MD 25 29, CAT. No: MD 25 29, CAT. No: GR 25 11; respectively. Acetylcholinesterase (AChE) ELISA Kit obtained from (Bioassay technology laboratory, Egypt) Cat. No: E0724Ra.

Total RNA Purification Kit following the manufacturer protocol, RNA extraction kit (Thermo Scientific, Fermentas, #K0731). Reverse transcription kits (Thermo Scientific, Fermentas, #EP0451). Primary antibodies for immunohistochemical examination: Rabbit anti-rat polyclonal phosphorylated Tau (P-Tau) antibody (Biosource International, Inc. USA) with a dilution of 1:50. Mouse anti-GFAP antibody (Cat. No. MS- 280- R7, Lab Vision Corporation, Fremont, USA) diluted in 1:100 in Lab Vision antibody diluent (Cat. TA- 125- UD).

3.1.2. Animals

In the current study, a total of 24 male Albino rats weighing approximately (180 \pm 10 g) were utilized. They were housed in four plastic cages at the Animal House of Zagazig University Faculty of Medicine.

3.1.3. Ethical approval

All animal procedures and experimental protocols were carried out in accordance with the Zagazig University Institutional Animal Care and Use Committee, Zagazig University (ZU-IACUC) guidelines under number of (ZU-IACUC/1/F/105/2019).

3.1.4. Experimental design

Following a two-week period of acclimation, the rats were divided into four equal groups, with six rats each. Group I (negative control group; cnt): healthy rats were fed a regular diet. Group II (positive control group; Dis): Rats were injected intraperitoneally (I.P.) with AlCl₃ at a dose of 40 mg/kg per day for 45 days [49]. Group III (protective group; pro): Rats received curcumin nanoparticles at a dose of 150 mg/kg orally via a gastric tube for four weeks [50]; following the first week of nanocurcumin, AlCl₃ was injected at a dose of 40 mg/kg/day for 45 days. Group IV (Nanocurcumin-treated group; Tre): Rats received daily AlCl₃ injection at a dose of 40 mg/kg/day for 45 days. After that, rats received daily oral doses of nanocurcumin, same as in group III, for an additional 4 weeks.

3.1.5. Sampling

At the end of the experiment and after performing the behavioral test, rats were euthanized by decapitation. After dissection, the whole brains were removed carefully, washed with saline, and divided in a sagittal plane into the following parts. Part I brain sections were fixed for 48 hours in 10% neutral buffered formalin, then they were cut to a thickness of 5 μ m, to be processed for both histological and immune-histochemical examinations [51]. Part II was stored in liquid nitrogen for gene expression analysis.

Preparation of tissue homogenate

Part III Brain tissue from each group was used to create tissue homogenates; brain tissue was kept in phosphate buffered saline solution (PBS) with a pH of 7.4. A glass porcelain homogenizer was used for 5 minutes to homogenize the tissue, and it was centrifuged for 15 minutes at 7000 \times g [52] used for estimating the biochemical estimations.

3.2. Methods

3.2.1. Synthesis of Curcumin-Loaded Chitosan-TPP Nanoparticles:

The process of ionotropic gelation was employed to encapsulate curcumin within chitosan nanoparticles [1:3]. Curcumin-Loaded Chitosan-TPP Nanoparticles were prepared and characterized by prof. dr. Yasser A. Atteia according to [53].

3.2.2. Behavioral Tests

The modified Barnes maze (MBM) technique used in this study was partially based on a previously published method Vargas-Lopez et al. [54]. It is constructed from a 122 cm diameter, raised (108 cm off the floor) circular black acrylic platform with twenty holes all around it. Only one of the holes is connected to a tunnel or black escape box, although they all have the same diameter (10 cm) and appearance. 38.7 cm in length, 12.1 cm in breadth, and 14.2 cm in depth are the dimensions of the detachable escape box. The white squared beginning chamber, an opaque, 20 cm x 30 cm long, 15 cm high, open-ended chamber, is used to set the rats on the platform. Four proximal visual cues are located throughout the room, each 50 centimeters from the circular platform. The escape hole was numbered 0 for the sake of graphic normalization, and the other holes were numbered 1 through 10 clockwise and -1 to -9 anticlockwise. To evaluate both recent and long-term spatial memory recall, we employed a modified protocol consisting of three days of acquisition trials (AT) followed by two probe trials (PT) one and five days following training. An AT involves placing a rat in the first chamber for thirty seconds, raising it, activating bright lights and high-pitched noises, and letting it explore the labyrinth for 120 seconds.

3.2.3. Assessment of antioxidants biomarkers in brain tissues

Reduced glutathione (GSH) level was estimated according to the method described by Beutler et al., [55], catalase (CAT) and Superoxide dismutase (SODs) activities were estimated according to Aebi [56], and Nishikimi et al., [57] methods; respectively.

3.2.4. Estimation of Acetyl Choline Esterase (AChE) activity

Acetylcholinesterase (AChE) activity was determined in brain tissue homogenates according to Ellman et al., protocol [58].

3.2.5. Quantitative real-time PCR (RT-PCR) analysis of Neurogranin (RC3) and β -amyloid precursor protein (APP) genes

RNA Purification Kits were utilized to ascertain the mRNA expression of the Neurogranin (RC3) and β -amyloid precursor protein (APP) genes. After total RNA was extracted from brain tissues using a (Thermo Scientific, Fermentas, #K0731) kit, RNA was transformed into complementary DNA (cDNA) using a genetically engineered M-MuLV RT (Thermo Scientific, Fermentas, #EP0451). Using a PCR equipment (Stratagene MX3005P) and SYBR Green PCR Master Mix (Quanti Tect SYBR Green real time PCR Kit; Thermo Scientific, USA, # K0221), semi-quantitative real-time PCR was carried out. The 2Ct method was used to assess the target genes' relative mRNA expression [59]. The primer sequences used were listed in Table 6.

Table 6: Forward and reverse primers sequence for primers used in qPCR

Gene	Primer sequence	Reference
APP	Forward primer (5' ----- /3) CAACCGTGGCATCCTTTTGG	[60]
	Reverse primer (5' ----- /3) CGTCGACAGGCTCAACTTCA	
RC3	Forward primer (5' ----- /3) CTCCAAGCCAGACGACGATATTC	[61]
	Reverse primer (5' ----- /3) CACTCTCCTGCCTTTATCTTCTTC	
β -actin	Forward primer (5' ----- /3) AAGTCCCTCACCCCTCCAAAAG	
	Reverse primer (5' ----- /3) AAGCAATGCTGTACCTTCCC	

3.2.6. Histological examination of Brain

Brain tissue sections were fixed in Bouin's solution, embedded in paraffin wax, cut into 5 μ m sections with a rotary microtome (SLEE technik- Germany). They were mounted on glass slides then stained with Hematoxylin and Eosin stain for routine histological examination.

3.2.7. Immunohistochemical examination

Anti-P-Tau and anti-GFAP antibodies were detected immunohistochemically utilizing the streptavidin–biotin complex immunoperoxidase method. Brain tissue sections were deparaffinized and placed on positively charged slides. They were then treated in 0.1% hydrogen peroxide for 30 minutes to inhibit the activity of endogenous peroxidase. Finally, the appropriate primary antibodies were incubated on the slides for an entire night. After several PBS washes, slices were incubated with a secondary antibody and a streptavidin–peroxidase conjugate for 30 minutes at room temperature. Following a five-minute incubation period with diaminobenzidine, sections were counterstained with Mayer's hematoxylin and washed with PBS. For the negative controls, PBS was utilized in place of the primary antibodies [62].

3.2.8. Morphometric study

The image analyzer computer system Leica Qwin 500 (Leica Ltd, Cambridge, UK) at the image analysis unit of Medical Histology and Cell Biology department, Faculty of Medicine, Zagazig University, using Fiji image J (1.51n, NIH, USA)

program to analyze the area % of immune-positive cells for P-TAU and GFAP. The interactive measure menu was used to measure them. Ten readings from five distinct areas from each rat in all groups were evaluated.

3.2.9. Statistical Analysis

The means \pm S.E. were used to express all of the data. One-way analysis of variance (ANOVA) was used to assess the statistical significance, and Duncan's multiple range test (DMRT) was used to generate individual comparisons using SPSS, 18.0 software from 2011. When $p < 0.05$, values were deemed statistically significant. To evaluate significance between groups, the test for the least significant difference (LSD) was also employed.

4. Conclusions

Nanocurcumin may be helpful in the prevention and treatment of AD since it reduces the toxicity of $AlCl_3$. Curcumin nano-formulations have revolutionized the treatment of diseases by improving cellular absorption, permeability with increased plasma levels, and bioavailability. Nano-formulations conjugated with curcumin have shown many benefits against neurodegeneration, and excellent encapsulating ability with improved physicochemical stability to penetrate against the blood-brain barrier suggesting that nanocurcumin is one of the most promising and exciting compounds for the development of AD therapeutics.

5. Conflicts of interest

There are no conflicts to declare.

6. Formatting of funding sources

No organization provided funding for the research, writing, or publication of this work, and the authors have no relevant financial or non-financial interests..

7. Acknowledgments

The authors greatly appreciate the support provided by Professor Dr. Yasser Attia and extend their sincere thanks and praise to him for his contribution to the research. National Institute of Laser Sciences, Cairo University, Giza, Egypt.

8. References and Bibliography

- [1] Qin, F.; Luo, M.; Xiong, Y.; Zhang, N.; Dai, Y.; Kuang, W.; and Cen, X. Prevalence and associated factors of cognitive impairment among the elderly population: A nationwide cross-sectional study in China. *Front. Public Health*, 2022, 10, 1032666. [doi:10.3389/fpubh.2022.1032666](https://doi.org/10.3389/fpubh.2022.1032666).
- [2] Shabbir, U.; Rubab, M.; Tyagi, A.; and Oh, D.-H. Curcumin and Its Derivatives as Theranostic Agents in Alzheimer's Disease: The Implication of Nanotechnology. *Int. J. Mol. Sci.*, 2021, 22, 196. [doi: https://dx.doi.org/10.3390/ijms22010196](https://dx.doi.org/10.3390/ijms22010196).
- [3] Kumar, A.; Sidhu, J.; Goyal, A.; Tsao, J.W.; and Doerr, C. Alzheimer Disease (Nursing). In *Stat Pearls*; Stat Pearls Publishing: Treasure Island, FL, USA, 2021. [PMID: 33760564](https://pubmed.ncbi.nlm.nih.gov/33760564/).
- [4] Wattmo, C.; Minthon, L.; and Wallin, A.K. Mild versus moderate stages of Alzheimer's disease: Three-year outcomes in a routine clinical setting of cholinesterase inhibitor therapy. *Alzheimer's Res. Ther.*, 2016, 17:8:7. [doi: 10.1186/s13195-016-0174-1](https://doi.org/10.1186/s13195-016-0174-1).
- [5] Armstrong, R.A. Risk factors for Alzheimer's disease. *Folia Neuropathol.*, 2019, 57, 87–105. [doi: 10.5114/fn.2019.85929](https://doi.org/10.5114/fn.2019.85929).
- [6] Colomina, M.T.; and Peris-Sampedro, F. Aluminum and Alzheimer's disease. *Adv. Neurobiol.*, 2017, 18, 183–197. [doi: 10.1007/978-3-319-60189-2_9](https://doi.org/10.1007/978-3-319-60189-2_9).
- [7] Pange, S.S.; Patwekar, M.; Patwekar, F.; Alghamdi, S.; Babalghith, A.O.; Abdulaziz, O.; Jawaid, T.; Kamal, M.; Tabassum, S.; and Mallick, J. A potential notion on Alzheimer's disease: nanotechnology as an alternative solution. *Journal of Nanomaterials*, 2022, vol. 2022, pp. 1–8. [doi:10.1155/2022/6910811](https://doi.org/10.1155/2022/6910811).
- [8] Hejazian, L.B.; Hosseini, S.M.; Taravati, A.; Asadi, M.; Bakhshi, M.; Nezhad, P.M.; Gol, M.; and Mououdi, M. Effect of Rosa damascena Extract on Rat Model Alzheimer's Disease: A Histopathological, Behavioral, Enzyme Activities, and Oxidative Stress Study. *Hindawi, Evidence-Based Complementary and Alternative Medicine*, 2023, Volume 2023, 11 pages. doi.org/10.1155/2023/4926151.
- [9] Oliveira, J.T.; and Pieniz, S. Curcumin in Alzheimer's Disease and Depression: Therapeutic Potential and Mechanisms of Action. *Brazilian Archives of Biology and Technology*. 2024, Vol.67: e24220004. [doi: 10.1590/1678-4324-2024220004](https://doi.org/10.1590/1678-4324-2024220004).
- [10] Zahran, F.; Mady, E.; Yasein, O.; and Keshta, A.T. Curcumin / BSA: New approach for hepatocellular carcinoma treatment. *BCAIJ*, 2014, 8(2), [51-60]. [Corpus ID: 20664869](https://www.researchgate.net/publication/26664869).
- [11] Anwar, S.K.; Elmonaem, S.N.A.; Moussa, E.; Aboulela, A.G.; and Essawy, M.M. Curcumin nanoparticles: The topical antimycotic suspension treating oral candidiasis. *Odontology*, 2023, 111(2):350-359. [doi: 10.1007/s10266-022-00742-4](https://doi.org/10.1007/s10266-022-00742-4).
- [12] Salah, A.; Yousef, M.; Kamel, M.; and Hussein, A. The Neuroprotective and Antioxidant Effects of Nanocurcumin Oral Suspension against Lipopolysaccharide-Induced Cortical Neurotoxicity in Rats. *Biomedicines*, 2022, 10, 3087. doi.org/10.3390/biomedicines10123087.
- [13] Karthikeyan, A.; Senthil, N.; and Min, T. Nanocurcumin: A promising candidate for therapeutic applications *Frontiers in Pharmacology*. 2020, 11: 487. [doi: 10.3389/fphar.2020.00487](https://doi.org/10.3389/fphar.2020.00487).

- [14] Martínez, N.N.; Hernández, J.T.; and Morales, J.O. Nanoparticles for the potential treatment of Alzheimer's disease: A physiopathological approach. *Nanotechnology Reviews*; 2023, 12 (1) 20220548. [doi: 10.1515/ntrev-2022-0548](https://doi.org/10.1515/ntrev-2022-0548).
- [15] Farkhondeh, T.; Samarghandian, S.; Pourbagher-Shahri, A.M.; and Sedaghat, M. The impact of curcumin and its modified formulations on Alzheimer's disease. *J. Cell. Physiol.*, 2019, 234 (10): 16953-16965. [doi: 10.1002/jcp.28411](https://doi.org/10.1002/jcp.28411).
- [16] Pange, S.S.; Patwekar, M.; Patwekar, F.; Alghamdi, S.; Babalghith, A.O.; Abdulaziz, O.; Jawaid, T.; Kamal, M.; Tabassum, S.; and Mallick, J. "A potential notion on Alzheimer's disease: nanotechnology as an alternative solution," *Journal of Nanomaterials*, 2022, vol. 2022, pp. 1–8. [doi:10.1155/2022/6910811](https://doi.org/10.1155/2022/6910811).
- [17] Singh, S.; Singh, R.; Kushwah, A.S.; and Gupta, G.; Neuroprotective role of antioxidant and pyranocarboxylic acid derivative against $AlCl_3$ induced Alzheimer's disease in rats. *Journal of Coastal Life Medicine*; 2014, 2(7): 571-578. [doi:10.12980/JCLM.2.2014J58](https://doi.org/10.12980/JCLM.2.2014J58).
- [18] Al Osman, M.; Yang, F.; and Massey, I.Y. Exposure routes and health effects of heavy metals on children. *Biometals.*; 2019, 32(4) : 563-573. [doi: 10.1007/s10534-019-00193-5](https://doi.org/10.1007/s10534-019-00193-5).
- [19] Patwekar, M.; Patwekar, F.; Mezni, A.; Sanaullah, S.; Rohin, S.F.; Almas, U.; Ahmad, I.; Tirth, V.; and Mallick, J. "Assessment of antioxidative and alpha-amylase potential of polyherbal extract. Evidence-based Complementary and Alternative Medicine, 2022, 22 (11):10. [doi: 10.1155/2022/7153526](https://doi.org/10.1155/2022/7153526).
- [20] Panzarini, E.; Mariano, S.; Tacconi, S.; Carata, E.; Tata, A.M.; and Dini, L. Novel therapeutic delivery of nanocurcumin in central nervous system related disorders. *Nanomaterials*. 2020, 11(1):2. [doi: 10.3390/nano11010002](https://doi.org/10.3390/nano11010002).
- [21] Helli, B.; Gerami, H.; Kavianpour, M.; Heybar, H.; Hosseini, S.K.; and Haghghian, H.K. Curcumin nanomicelle improves lipid profile, stress oxidative factors and inflammatory markers in patients undergoing coronary elective angioplasty; A randomized clinical trial. *Endocr Metab Immune Disord Drug Targets*. 2021, 21(11):2090-2098. [doi: 10.2174/1871530321666210104145231](https://doi.org/10.2174/1871530321666210104145231).
- [22] Abduljawad, A.A.; Elawad, M.A.; Elkhalifa, M.E.M.; Ahmed, A.; Hamdoon, A.A.E; Salim, L.H.M.; Ashraf, M.; Ayaz, M.; Hassan, S.S.Ul.; and Bungau, S. Alzheimer's disease as a major public health concern: Role of dietary saponins in mitigating neurodegenerative disorders and their underlying mechanisms. *Molecules.*, 2022, 27(20): 6804. [doi: 10.3390/molecules27206804](https://doi.org/10.3390/molecules27206804).
- [23] Li, J.; Yang, J.Y.; Yao, X.C.; Xue, X.; Zhang, Q.C.; Wang, X.X.; Ding, L.L.; and Wu, C.F. Oligomeric Abeta-induced microglial activation is possibly mediated by NADPH oxidase. *Neurochem Res.*, 2012, 38(2):443-452. doi.org/10.1007/s11064-012-0939-2.
- [24] Tsai, Y.M.; Chien, C.F.; Lin, L.C.; and Tsai, T.H. Curcumin and its nano-formulation: The kinetics of tissue distribution and blood-brain barrier penetration. *Int. J. Pharm.*, 2011, 416 (1): 331–338. [doi: 10.1016/j.ijpharm.2011.06.030](https://doi.org/10.1016/j.ijpharm.2011.06.030).
- [25] Rajasekar, A. Facile synthesis of curcumin nanocrystals and validation of its antioxidant activity against circulatory toxicity in Wistar rats. *J. Nanosci. Nanotechnol.*, 2015, 15, 4119–4125. [doi: 10.1166/jnn.2015.9600](https://doi.org/10.1166/jnn.2015.9600).
- [26] Fakhri, S.; Alizadeh, A.; and Shahryari, A. Effect of 6 Weeks of High Intensity Interval Training with Nano-curcumin Supplement on Antioxidant Defence and Lipid Peroxidation in Overweight Girls-Clinical Trial. *Iranian J. Diabetes Obesity*, 2019, 11, 173–180. [doi: 10.18502/ijdo.v11i3.2606](https://doi.org/10.18502/ijdo.v11i3.2606).
- [27] Kahya, M.C.; Naziroğlu, M.; and Övey, İ.S. Modulation of Diabetes-Induced Oxidative Stress, Apoptosis, and Ca^{2+} Entry Through TRPM2 and TRPV1 Channels in Dorsal Root Ganglion and Hippocampus of Diabetic Rats by Melatonin and Selenium. *Mol Neurobiol.*, 2017, 54 (3):2345-2360. [doi: 10.1007/s12035-016-9727-3](https://doi.org/10.1007/s12035-016-9727-3).
- [28] Zhang, W.; Huang, Q.; Zeng, Z.; Wu, J.; Zhang, Y.; and Chen, Z. Sirt1 inhibits oxidative stress in vascular endothelial cells. *Oxid Med Cell Longev.*, 2017, 7543973. [doi: 10.1155/2017/7543973](https://doi.org/10.1155/2017/7543973).
- [29] Rinne, J.O.; Kaasinen, V.; Järvenpää, T.; Nägren, K.; Roivainen, A.; Yu, M.; Oikonen, V.; and Kurki, T. Brain acetylcholinesterase activity in mild cognitive impairment and early Alzheimer's disease. *J Neurol Neurosurg Psychiatry.*, 2023, 74:113–115. [doi: 10.1136/jnnp.74.1.113](https://doi.org/10.1136/jnnp.74.1.113).
- [30] Wong, X.Y.; Sena-Torrallba, A.; Álvarez-Diduk, R.; Muthoosamy, K.; and Merkoçi, A. Nanomaterials for nanotheranostics: Tuning their properties according to disease needs. *ACS Nano.*, 2020, 14 (3), 2585–2627. [doi:10.1021/acsnano.9b08133](https://doi.org/10.1021/acsnano.9b08133).
- [31] M'rad, I.; Jeljeli, M.; Rihane, N.; Hilber, P.; Sakly, M.; and Amara, S. Aluminium oxide nanoparticles compromise spatial learning and memory performance in rats. *Excli Journal.*, 2018, 17:200-210. [doi: 10.17179/excli2017-1050](https://doi.org/10.17179/excli2017-1050).

- [32] Lakshmi, B.V.S.; Sudhakar, M.; and Prakash, K.S. Protective effect of selenium against aluminum chloride-induced Alzheimer's Disease: behavioral and biochemical alterations in rats. *Biol Trace Elem Res.*, 2015, 165 (1):67-74. [doi: 10.1007/s12011-015-0229-3](https://doi.org/10.1007/s12011-015-0229-3).
- [33] Thakur, S.; Dhapola, R.; Sarma, P.; Medhi, B.; and Reddy, D.H. Neuroinflammation in Alzheimer's disease: Current progress in molecular signalling and therapeutics. *Inflammation*, 2023, 46 (1), 1–17. [doi:10.1007/s10753-022-01721-1](https://doi.org/10.1007/s10753-022-01721-1).
- [34] Liu W., Lin H., He X., Chen L., Dai Y., Jia W., Xue X., Tao J. and Chen L. Neurogranin as a cognitive biomarker in cerebrospinal fluid and blood exosomes for Alzheimer's disease and mild cognitive impairment. *Translational Psychiatry*. 2020, 10, 125. [doi: 10.1038/s41398-020-0801-2](https://doi.org/10.1038/s41398-020-0801-2).
- [35] Agnello, L.; Lo Sasso, B.; Vidali, M.; Scazzone, C.; Piccoli, T.; Gambino, C.M.; Bivona, G.; Giglio, R.V.; Ciaccio, A.M.; La Bella, V. et al., Neurogranin as a Reliable Biomarker for Synaptic Dysfunction in Alzheimer's Disease. *Diagnostics*, 2021, 11, 2339. doi.org/10.3390/diagnostics11122339.
- [36] Stillman, M.D.; Barber, J.; Burns, S.; Williams, S.; and Hoffman, J.M. Complications of spinal cord injury over the first year after discharge from inpatient rehabilitation. *Archives of Physical Medicine and Rehabilitation*. 2017, 98(9):1800-1805. [doi: 10.1016/j.apmr.2016.12.011](https://doi.org/10.1016/j.apmr.2016.12.011).
- [37] Yang, R.; Zheng, Y.; Wang, Q.; and Zhao, L. Curcumin-loaded chitosan–bovine serum albumin nanoparticles potentially enhanced A β 42 phagocytosis and modulated macrophage polarization in Alzheimer's disease. *Nanoscale Res. Lett.*, 2018, 13 (1), 330. [doi:10.1186/s11671-018-2759-z](https://doi.org/10.1186/s11671-018-2759-z).
- [38] Eghbaliferiz, S.; Farhadi, F.; Barreto, G.E.; Majeed, M.; Sahebkar, A. Effects of curcumin on neurological diseases: focus on astrocytes. *Pharmacological Reports.*, 2020, 72(4):769-782. [doi: 10.1007/s43440-020-00112-3](https://doi.org/10.1007/s43440-020-00112-3).
- [39] Saunders, T.; Gunn, C.; Blennow, K.; Kvartsberg, H.; Zetterberg, H.; Shenkin, S.D.; Cox, S.R.; Deary, I.J.; Smith, C.; King, D.; and Spiers-Jones, T. Neurogranin in Alzheimer's disease and ageing: A human post-mortem study. *Neurobiology of Disease*. 2023, 177:105991. [doi: 10.1016/j.nbd.2023.105991](https://doi.org/10.1016/j.nbd.2023.105991).
- [40] Sokolow, S.; Henkins, K.M.; Bilousova, T.; Gonzalez, B.; Vinters, H.V.; Miller, C.A.; et al., Pre-synaptic C-terminal truncated tau is released from cortical synapses in Alzheimer's disease. *J. Neurochem.*, 2015, 133(3):368-79. [doi: 10.1111/jnc.12991](https://doi.org/10.1111/jnc.12991).
- [41] Akhtar, A.; Bishnoi, M.; and Sah, S.P. Sodium orthovanadate improves learning and memory in intra-cerebroventricular-streptozotocin rat model of Alzheimer's disease through modulation of brain insulin resistance induced tau pathology. *Brain Res. Bull.*, 2020, 164: 83–97. [doi: 10.1016/j.brainresbull.2020.08.001](https://doi.org/10.1016/j.brainresbull.2020.08.001).
- [42] Ossenkoppele, R.; van der Kant, R.; and Hansson, O. Tau biomarkers in Alzheimer's disease: towards implementation in clinical practice and trials. *The Lancet Neurology.*, 2022, 21(8):726-734. [doi: 10.1016/S1474-4422\(22\)00168-5](https://doi.org/10.1016/S1474-4422(22)00168-5).
- [43] Sun, J.; Zhang, X.; Wang, C.; Teng, Z.; and Li, Y. Curcumin decreases hyperphosphorylation of tau by down-regulating caveolin-1/GSK-3 β in N2a/APP695SWE cells and APP/PS1 double transgenic Alzheimer's disease mice. *Am J Chin Med.*, 2017, 45(8):1667–1682. [doi: 10.1142/S0192415X17500902](https://doi.org/10.1142/S0192415X17500902).
- [44] Yang, Z.; and Wang, K.K. Glial fibrillary acidic protein: from intermediate filament assembly and gliosis to neurobiomarker. *Trends in Neurosciences*. 2015, 38(6):364-74. [doi: 10.1016/j.tins.2015.04.003](https://doi.org/10.1016/j.tins.2015.04.003).
- [45] Jurga, A.M.; Paleczna, M.; Kadluczka, J.; and Kuter, K.Z. Beyond the GFAP-astrocyte protein markers in the brain. *Biomolecules*, 2021, 11 (9):1361. doi.org/10.3390/biom11091361.
- [46] Oeckl, P.; Halbgebauer, S.; Anderl-Straub, S.; Steinacker, P.; Huss, A.M.; Neugebauer, H.; von Arnim, C.A.F.; Diehl-Schmid, J.; Grimmer, T.; Kornhuber, J.; Lewczuk, P.; Danek, A.; et al., Glial fibrillary acidic protein in serum is increased in Alzheimer's disease and correlates with cognitive impairment. *J Alzheimers Dis.*, 2019, 67(2):481-488. [doi: 10.3233/JAD-180325](https://doi.org/10.3233/JAD-180325).
- [47] Betcher, B.M.; Olson, K.E.; Carlson, N.E.; McConnell, B.V.; Boyd, T.; Adame, V.; Solano, D.A.; Anton, P.; Markham, N.; Thaker, A.A.; Jensen, A.M.; Dallmann, E.N.; Potter, H.; and Coughlan, C. Astroglialosis and episodic memory in late life: higher GFAP is related to worse memory and white matter microstructure in healthy aging and Alzheimer's disease. *Neurobiol Aging.*, 2021, 103:68-77. doi.org/10.1016/j.neurobiolaging.2021.02.012.
- [48] Mohammadi, A.; Colagar, A.H.; Khorshidian, A.; and Amini, S.M. The Functional roles of curcumin on astrocytes in neurodegenerative diseases. *Neuroimmunomodulation*. 2022, 29 (1):4-14. [doi: 10.1159/000517901](https://doi.org/10.1159/000517901).
- [49] Thenmozhi, A.J.; Dhivyabharathi, M.; Raja, W.T.R.; Manivasagam, T.; and Essa, M.M. Tannoid principles of *Embolia officinalis* renovate cognitive deficits and attenuate amyloid pathologies against aluminum

- chloride induced rat model of Alzheimer's disease. *Nutr Neurosci.* 2016 19: 269–278. doi: [10.1179/1476830515Y.0000000016](https://doi.org/10.1179/1476830515Y.0000000016).
- [50] Khatri, D.K.; and Juvekar, A.R. Neuroprotective effect of curcumin as evinced by abrogation of rotenone-induced motor deficits, oxidative and mitochondrial dysfunctions in mouse model of Parkinson's disease. *Pharmacol Biochem Behav.*, 2016,150-151:39-47. doi: [10.1016/j.pbb.2016.09.002](https://doi.org/10.1016/j.pbb.2016.09.002).
- [51] Bancroft, J.; Stevens, A.; and Turner, D. *Theory and Practice of Histological Techniques*, fourth ed. Churchill Livingstone, New York, Edinburgh, Madrid, San Francisco, 1996, p. 20.
- [52] Keshta, A.T.; Fathallah, A.M.; Attia, Y.A.; Salem, E.A.; and Watad, S.H. Ameliorative effect of selenium nanoparticles on testicular toxicity induced by cisplatin in adult male rats. *Food and Chemical Toxicology.* 2023. Volume 179, Page 113979. doi: [10.1016/j.fct.2023.113979](https://doi.org/10.1016/j.fct.2023.113979).
- [53] Nair, R.S.; Morris, A.; Billa, N.; and Leong, C.O. An evaluation of curcumin-encapsulated chitosan nanoparticles for transdermal delivery. *Aaps PharmSciTech.* 2019, 20 (2): 69. doi: [10.1208/s12249-018-1279-6](https://doi.org/10.1208/s12249-018-1279-6).
- [54] Vargas-López, V.; Lamprea, M.R.; and Múnera, A. Characterizing spatial extinction in an abbreviated version of the Barnes maze. *Behav Proc.*;2011, 86:30–38. doi: [10.1016/j.beproc.2010.08.002](https://doi.org/10.1016/j.beproc.2010.08.002).
- [55] Beutler, E.; Duron, O.; and Kelly, B.M. Improved method for the determination of blood glutathione. *J. Lab Clin. Med.* 1963, 61: 882. PMID: [13967893](https://pubmed.ncbi.nlm.nih.gov/13967893/).
- [56] Aebi, H.; Catalase in vivo. *Methods Enzymol.*, 1984, 105:121-6. doi: [10.1016/s0076-6879\(84\)05016-3](https://doi.org/10.1016/s0076-6879(84)05016-3).
- [57] Nishikimi, M.; Roa, N.A.; and Yogi, K. The occurrence of superoxide anion in the reaction of reduced phenazine methosulfate and molecular oxygen. *Biochem Biophys Res Commun.*, 1972, 46(2):849-54. doi: [10.1016/s0006-291x\(72\)80218-3](https://doi.org/10.1016/s0006-291x(72)80218-3).
- [58] Ellman, G.L.; Courtney, K.D.; Andres, Jr V.; and Featherstone, R.M. A new and rapid colorimetric determination of acetylcholinesterase activity. *Biochemical Pharmacology.* 1961, 7:88-95. doi: [10.1016/0006-2952\(61\)90145-9](https://doi.org/10.1016/0006-2952(61)90145-9).
- [59] Livak, K.J.; and Schmittgen, T.D. Analysis of relative gene expression data using real-time quantitative PCR and the 2⁻ΔΔCT method. *Methods.*, 2001, 25(4):402-8. doi: [10.1006/meth.2001.1262](https://doi.org/10.1006/meth.2001.1262).
- [60] Zimmermann, B.; Holzgreve, W.; Wenzel, F.; and Hahn, S. Novel Real-Time Quantitative PCR Test for Trisomy 21. *Clin Chem.*, 2002, 48, (2): 362-363. doi: [10.1093/clinchem/48.2.362](https://doi.org/10.1093/clinchem/48.2.362).
- [61] Calkins, M.J.; Manczak, M.; Mao, P.; Shirendeb, U.; and Reddy, P.H. Impaired mitochondrial biogenesis, defective axonal transport of mitochondria, abnormal mitochondrial dynamics and synaptic degeneration in a mouse model of Alzheimer's disease. *Human Molecular Genetics.* 2011, 20, (23):4515–4529. doi: [10.1093/hmg/ddr381](https://doi.org/10.1093/hmg/ddr381).
- [62] Ramos-Vara, J.A.; Kiupel, M.; Baszler, T.; Bliven, L.; Brodersen, B.; Chelack, B.; Czub, S.; Del Piero, F.; Dial, S.; Ehrhart, E.J.; Graham, T.; Manning, L.; Paulsen, D.; Valli, V.E.; and West, K. Suggested guidelines for immunohistochemical techniques in veterinary diagnostic laboratories. *Journal of Veterinary Diagnostic Investigation.*; 2008, 20 (4):393-413. doi: [10.1177/104063870802000401](https://doi.org/10.1177/104063870802000401).